Successive phase transitions at finite temperatures toward the supersolid state in a three-dimensional extended Bose-Hubbard model

Keisuke Yamamoto,[1] Synge Todo,[2,3] and Seiji Miyashita[1,3]
[1]*Department of Physics, School of Science, The University of Tokyo, 7-3-1 Hongo, Bunkyo-ku, Tokyo 113-0033, Japan*
[2]*Department of Applied Physics, School of Engineering, The University of Tokyo, 7-3-1 Hongo, Bunkyo-ku, Tokyo 113-8656, Japan*
[3]*CREST, JST, 4-1-8 Honcho Kawaguchi, Saitama 332-0012, Japan*
(Received 9 July 2008; published 3 March 2009)

We study the finite temperature properties of the extended Bose-Hubbard model on a cubic lattice. This model exhibits the so-called supersolid state. To start with, we investigate the ground-state phase diagram and find the supersolid state in the region of underdoped (less than the half-filled) density in contrast to the cases of one- and two-dimensional systems where the superfluid state and the solid state show the phase separation. Next, we investigate ordering processes at finite temperatures by quantum Monte Carlo simulations and find successive superfluid and solid phase transitions. There, we find that the two order parameters compete with each other. We establish a finite temperature phase diagram, which contains the superfluid, the solid, the supersolid, and the disordered phases. We develop a mean-field theory to analyze the ordering processes and compare the result with that obtained by simulations and discuss the mechanism of the competition of these two orders. We also study how the supersolid region shrinks as the on-site repulsion becomes strong.

DOI: 10.1103/PhysRevB.79.094503 PACS number(s): 67.80.kb, 75.40.Mg, 02.60.−x, 64.60.−i

I. INTRODUCTION

The supersolid state is an interesting state of matter which has both solid and superfluid properties. The solid state is characterized by the breaking of translational symmetry and the superfluid state is characterized by the breaking of $U(1)$ symmetry of the phase of macroscopic wave function. Thus, the simultaneous breaking of these two symmetries indicates that there is a flow component in solid. The possibility of the supersolid was first discussed by Penrose and Onsager.[1] Since then, various studies on supersolid have been conducted from both experimental and theoretical points of view.

As to observation of supersolid, Leggett[2] suggested that nonclassical rotational inertia (NCRI) would be available to detect supersolid in rotating solid ^{4}He. Recently, Kim and Chan[3] reported that they found NCRI in solid ^{4}He. Although it has been pointed out that the observed NCRI may not be due to the supersolid but due to the grain boundaries between polycrystals,[4] the topic, however, still attracts researchers' interest.

The possibility of supersolid on lattice models has been discussed actively. Andreev and Lifshitz[5] suggested that the delocalization of the vacancies in crystal causes a mass flow. Matsuda and Tsuneto[6] studied the ground state of the hard-core Bose-Hubbard model using mean-field theory and they showed that the supersolid is possible when the interaction of particles has frustration. Numerically, it is shown that the hardcore Bose-Hubbard model on a triangular lattice has the supersolid phase, which shows a $\sqrt{3}\times\sqrt{3}$ structure and a finite superfluid fraction simultaneously.[7–11] Other frustrated lattices have been also studied[12,13] and they show the supersolid state.

Recently, it has been pointed out that the supersolid state can be realized even on nonfrustrated lattices if double occupancy of the particles is allowed.[14] In the case of a square lattice, the supersolid is found in the ground state when the number density of particle is more than that of the half-filled case ($\rho>1/2$).[14] The supersolid state in this density region is considered to be the delocalization state of the additional particles on the $\rho=1/2$ checkerboard solid. On the contrary, in the underdoped density region ($\rho<1/2$), the system shows a phase separation of the superfluid state and the solid state and the supersolid phase does not exist in one- and two-dimensional systems.[14] In the mean-field theory, however, the supersolid phase exists also in this region. In the present paper, first we investigate the existence of the supersolid phase in the underdoped density region by a quantum Monte Carlo method [the stochastic series-expansion (SSE) method[15,16]] and confirm that it indeed exists in the three-dimensional case.

So far, no direct study has been done on finite temperature properties of supersolid problem in the extended Bose-Hubbard model. It is an interesting problem to study how the orders of the superfluid and of the solid appear at finite temperatures when the system has the supersolid state in the ground state. In the model, the hopping term causes the superfluid order and the nearest-neighbor repulsive interaction tends to form the solid order. These orders compete with each other, and in the hardcore limit, these orders cannot be realized simultaneously. In the present paper, we investigate ordering processes of superfluid and solid at finite temperatures in the soft-core extended Bose-Hubbard model on a cubic lattice using SSE method. We establish a phase diagram of superfluid, normal solid, disordered state, and supersolid. We also study the finite temperature dependence of the orders by making use of mean-field (MF) analysis and compare the result to that obtained by SSE. They show qualitatively good agreement. Moreover, the competition of the solid and superfluid orders is discussed using Ginzburg-Landau free energy. Finally, we study effects of on-site repulsion U on the coexistence of the two orders. We find how the supersolid region at finite temperature shrinks as U becomes large.

II. MODEL

We analyze the extended Bose-Hubbard Hamiltonian on a cubic lattice

$$\mathcal{H} = -t\sum_{\langle ij\rangle}(a_i^\dagger a_j + a_i a_j^\dagger) + V\sum_{\langle ij\rangle} n_i n_j + \frac{1}{2}U\sum_i n_i(n_i-1) - \mu\sum_i n_i, \quad (1)$$

where $a_i^\dagger$ and a_i are the creation and annihilation operators of a boson ($[a_i, a_j^\dagger]=\delta_{ij}$) and $n_i=a_i^\dagger a_i$. The parameter t denotes the hopping matrix element, U and V are the on-site and nearest-neighbor repulsions, respectively, and μ is the chemical potential. The notation $\langle ij\rangle$ means the sum over the nearest-neighbor pairs. The system size is $N=L^3$, where L is the length of the system. The order parameter of the solid state is

$$S_\pi = \frac{1}{N^2}\sum_{jk} e^{i\mathbf{Q}\cdot(\mathbf{r}_j-\mathbf{r}_k)}\langle n_j n_k\rangle, \quad (2)$$

where $\mathbf{Q}=(\pi,\pi,\pi)$ is the wave vector that represents the staggered order. As for the order parameter of the superfluid state, we adopt Bose-Einstein condensation fraction

$$\rho_{k=0} = \frac{1}{N^2}\sum_{jk}\langle a_j^\dagger a_k + a_k^\dagger a_j\rangle \quad (3)$$

in the mean-field analysis, while in the SSE simulation we adopt the superfluidity ρ_s for the convenience of numerical calculation. The expression of ρ_s is given in Sec. III. Although these two quantities are not the same, both of them describe the off-diagonal long-range order (ODLRO) and are considered to represent the same qualitative nature of the superfluidity.

III. METHODS

We use the following two different methods to analyze properties of the system.

A. Stochastic series expansion

We perform numerical simulation of the SSE, which was invented by Sandvik.[15,16] This method is one of quantum Monte Carlo (QMC) simulations and has been successfully applied for various quantum systems. In order to avoid the clusterization due to diagonal frustration, we adopt the generalized directed loop algorithm.[17] We use a package of the Algorithms and Libraries for Physics Simulations (ALPS).[18,19] We adopt a simple-cubic lattice of $N=L^3$ sites with periodic boundary conditions along all the lattice axes. In the simulation, instead of the condensation fraction $\rho_{k=0}$ [Eq. (3)], we calculate superfluidity ρ_s using the winding number W of world lines[20,21]

$$\rho_s = \frac{\langle W^2\rangle}{3t\beta L}, \quad (4)$$

where β is the inverse temperature.

B. Mean-field approximation

We also analyze the ordering processes by the MF approximation.[22] In order to study the solid state, we use a sublattice structure which is characterized by a staggered order of the density. Here we adopt mean fields for the solid order and superfluid order at sublattices A and B. The Hamiltonian for this MF is given by

$$\mathcal{H}_{\mathrm{MF}} = \mathcal{H}_A + \mathcal{H}_B + C, \quad (5)$$

$$\mathcal{H}_A = -zt(a_A^\dagger + a_A)\phi_B + zVn_A m_B + \frac{U}{2}n_A(n_A-1) - \mu n_A, \quad (6)$$

$$\mathcal{H}_B = -zt(a_B^\dagger + a_B)\phi_A + zVn_B m_A + \frac{U}{2}n_B(n_B-1) - \mu n_B, \quad (7)$$

$$C = 2zt\phi_A\phi_B - zVm_A m_B, \quad (8)$$

where $z(=6)$ is the number of nearest-neighbor sites. Here, m_A and m_B are the mean fields corresponding to the expectation values of the number operators for A and B sites, respectively,

$$m_A = \langle n_A\rangle \quad \text{and} \quad m_B = \langle n_B\rangle. \quad (9)$$

Similarly, ϕ_A and ϕ_B correspond to the expectation values of the annihilation operators for A and B sites, respectively,

$$\phi_A = \langle a_A\rangle \quad \text{and} \quad \phi_B = \langle a_B\rangle. \quad (10)$$

Here, the expectation values are taken over the ground state in the case of $T=0$. In the finite temperature case, these represent the thermal averages.

$\mathcal{H}_A$ ($\mathcal{H}_B$) is a mean-field Hamiltonian at a site of the A (B) sublattice. C is a correction term compensating the double counting of the energy.

In the finite temperature case, the partition function and the free energy are given by

$$\mathcal{Z}_{\mathrm{MF}} = \mathrm{Tr}(e^{-\beta\mathcal{H}_{\mathrm{MF}}}), \quad (11)$$

$$F_{\mathrm{MF}} = -\frac{1}{\beta}\ln\mathcal{Z}_{\mathrm{MF}}. \quad (12)$$

In MF, $m\equiv(m_A-m_B)/2$ denotes the order parameter of solid and fulfill the relation $S_\pi=m^2$. Similarly, $\phi\equiv(\phi_A+\phi_B)/2$ represents the order parameter of superfluid and fulfill the relation, $\rho_{k=0}=2\phi^2$, according to Eq. (3).

IV. GROUND-STATE PROPERTIES

Before analyzing properties at finite temperatures, let us summarize the ground-state properties. As has been reported, the system may have the supersolid phase in the ground state when U takes a finite value.[14,23] In Fig. 1, we show the ground-state phase diagram in the coordinate of $(t/U, \mu/U)$ obtained by MF method. As for the supersolid state in the

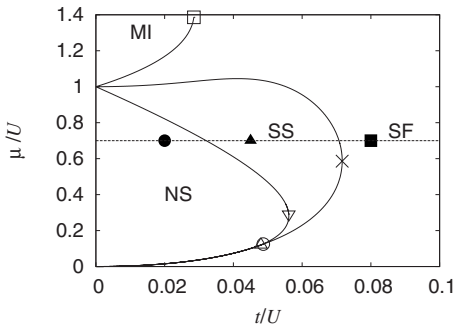

FIG. 1. The ground-state phase diagram of the soft-core Bose-Hubbard model for $V=U/z$ obtained by MF. There are four phases: NS, SS, SF, and MI. Characteristic points of the phase diagram are denoted by the common symbols in Fig. 2: open rectangle, cross, open downward triangle, open upward triangle, and open circle (see text). Temperature dependence of order parameters calculated by SSE is given in Fig. 5 at the positions denoted by solid circle, solid triangle, and solid rectangle.

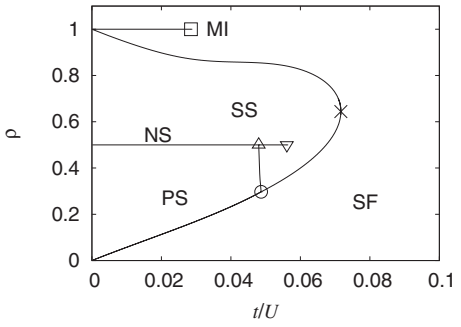

FIG. 2. The ground-state phase diagram in the coordinate of t/U and ρ for $V=U/z$. NS and MI are on the $\rho=1/2$ and $\rho=1$ lines, respectively. Characteristic points of the phase diagram are denoted by the common symbols in Fig. 1: open rectangle, cross, open downward triangle, open upward triangle, and open circle (see the text). In this coordinate, there appears a region of the PS for $\rho<1/2$.

region of $\rho>1/2$, we may have a picture that additional particles move on the commensurate solid structure. Let us consider a solid in which the sublattice A is occupied. There, effective potential energies for the additional particle on the A and B sublattices are U and zV, respectively. In the case $V=U/z$, the additional particles feel a flat potential and we expect that the fluidity of the particle is mostly enhanced. Indeed it is confirmed that the superfluidity takes maximum value at this ratio.[24] We adopt this ratio in the present study except in the final part of Sec. V. This choice of the ratio, however, does not cause qualitative change of the structure of the phase diagram.

In Fig. 1, the solid line is the phase boundary obtained by MF at $T=0$. This ground-state phase diagram agrees well with that obtained by the Gutzwiller variational method by van Otterlo *et al.*[23] We find four different phases, i.e., Mott-insulator (MI), normal solid (NS), superfluid (SF), and supersolid (SS). In addition to these four phases, a disordered phase representing the normal liquid (NL) phase appears at finite temperatures. We also study the ground states for several parameter sets by SSE. For example, we find the solid state for the set $(t/U=0.02, \mu/U=0.7)$ denoted by the solid circle in Fig. 1, the superfluid state for $(t/U=0.08, \mu/U=0.7)$ by the solid rectangle, and the supersolid state for $(t/U=0.045, \mu/U=0.7)$ by the solid triangle. The temperature dependences of order parameters on these points are given in Sec. V in Figs. 5(a)–5(c).

In order to understand the phase diagram as a function of the density ρ, we also give the phase diagram in the coordinate of t/U and ρ in Fig. 2. It is found that the normal solid and Mott-insulator phases are realized at commensurate density, i.e., $\rho=1/2$ and $\rho=1$, respectively. In this coordination, as well known, we have a domain denoted by PS which denotes the phase separation of solid and superfluid.[14] In order to make the comparison of the two phase diagrams, we plot some points in the phase diagrams with the same symbols. For example, the end point of MI is plotted by an open square in each phase diagram. Similarly, the end points of SS and NS are plotted by a cross and an open downward triangle, respectively. The phase transition between SF and NS is of the first order, which is manifested by the existence of PS in Fig. 2.

Here, it should be noted on the problem of the existence of the supersolid phase in the region of $\rho<1/2$. The boundary between PS and SS is not vertical. The end points of this border are plotted by an open upward triangle and an open circle. In Fig. 1, these two points are located very closely. Between them, we find the first-order phase transition between SF and SS. Although this underdoped supersolid state has been observed in the mean-field calculation,[23,25] the presence of this phase has been denied in one- and two-dimensional systems by the studies of quantum Monte Carlo method.[14,26] Here we study this problem in three dimensions using SSE.

We searched parameter sets in which the supersolid state exists in the region of $\rho<1/2$ and found that it really exists in some region of parameter sets. In Fig. 3, we show the μ dependence of density and order parameters for $t/U=0.055$. At $\mu/U=0.25$, the order parameters of the solid and the superfluid both remain finite, in contrast to the cases of the phase separation where either of them disappears. In Fig. 4, we show the size dependence of the solid and the superfluid order parameters for $t/U=0.055$ and $\mu/U=0.25$. The two order parameters converge to finite values keeping the den-

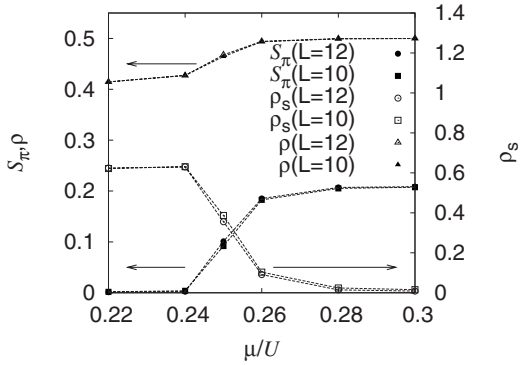

FIG. 3. Dependence of order parameters and density on μ for $(t/U=0.055, V=U/z)$. System sizes are $L=10$ and $L=12$.

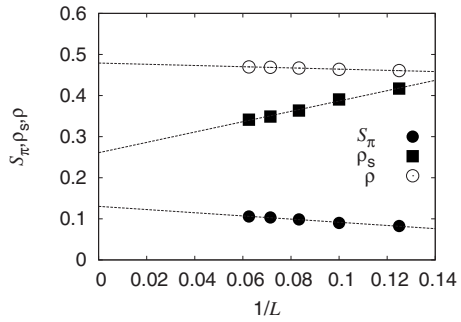

FIG. 4. The size dependence of the solid and the superfluid order parameters for the parameter set $(t/U=0.055, \mu/U=0.25, V=U/z)$ calculated by SSE. System sizes are from $L=8$ to $L=16$. Dashed lines denote linear extrapolations of data points.

sity $\rho<1/2$. Therefore we confirm the existence of the supersolid phase in the region of $\rho<1/2$.

V. PHASE TRANSITIONS AT FINITE TEMPERATURES

Now, we study the ordered states at finite temperatures. The phase transition between the normal liquid phase and the solid phase is expected to belong to the universality class of the Ising model because the phase transition occurs in the spontaneous symmetry breaking of the order parameter with the symmetry of Z_2. On the other hand, the phase transition of superfluid is expected to belong to the XY universality class because the order parameter has the symmetry of $U(1)$. In this section, we study the temperature dependence of these order parameters.

A. Stochastic series expansion

First, we show the results obtained by SSE. The simulations were performed in the grand canonical ensemble using a system sizes $N=10^3$ and $N=12^3$.

We plot the order parameters of solid, S_π, and that of superfluid, ρ_s, as a function of temperature for various values of t. In Fig. 5(a), we show the transition from normal liquid to normal solid for $t/U=0.02$ in which only S_π appears continuously. In the same way, the transition from normal liquid to superfluid for $t/U=0.08$ is depicted in Fig. 5(b). For $t/U=0.045$, the system shows successive transitions and the supersolid state is realized at low temperatures. There, we find that the solid order appears at a higher temperature [Fig. 5(c)]. Note that the solid order is suppressed when the superfluid order appears. Thus, we expected that the solid fraction and the superfluid fraction compete with each other. It should be noted that ρ_s appears at higher temperature than the solid order for $t/U=0.055$ (not shown).

In Fig. 6, we depict a phase diagram in the coordinate of $(t/U, T/U)$ for the fixed values $V/U=1/z$ and $\mu/U=0.7$. The transition temperatures of the solid state T_{S_π} are plotted by solid circles and those of the superfluid state T_{ρ_s} are plotted by open circles. To determine the transition temperatures for each value of t, we use the method of the Binder parameter[27] of the systems with $L=10$ and 12. In Fig. 6, there are four different phases: NL, NS, SF, and SS. These phases meet at a

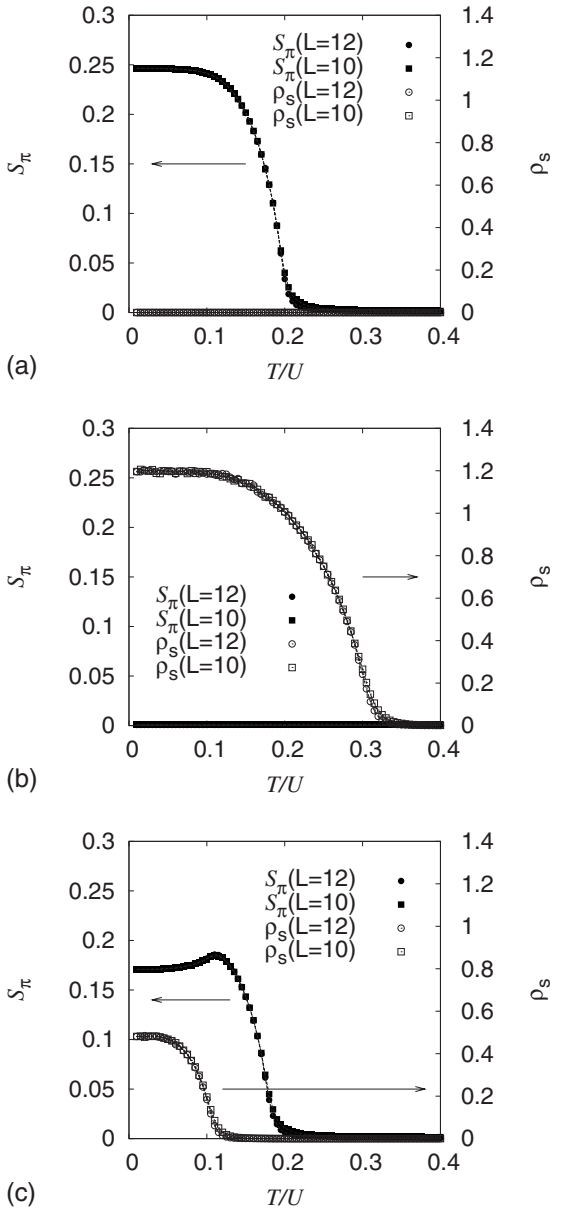

FIG. 5. Temperature dependence of order parameters obtained by SSE $(V=U/z)$. (a) $(t/U=0.02, \mu/U=0.7)$: normal liquid-normal solid transition. (b) $(t/U=0.08, \mu/U=0.7)$: normal liquid-superfluid transition. (c) $(t/U=0.045, \mu/U=0.7)$: normal liquid-normal solid transition and normal solid-supersolid transition.

tetracritical point (t_c, T_c). The competition of solid and superfluid orders is also found in the phase diagram (Fig. 6). Namely, above t_c, the transition temperature of solid is smaller than that of smooth extension of T_{S_π} from $t<t_c$. Therefore we conclude that T_{S_π} is suppressed from that of the case in which the superfluid would not order. Similarly, below t_c, the transition temperature of superfluid is smaller than that of the case in which the solid would not order.

B. Mean-field analysis

Here, we calculate the temperature dependence of order parameters by making use of MF. In Fig. 7, we show the

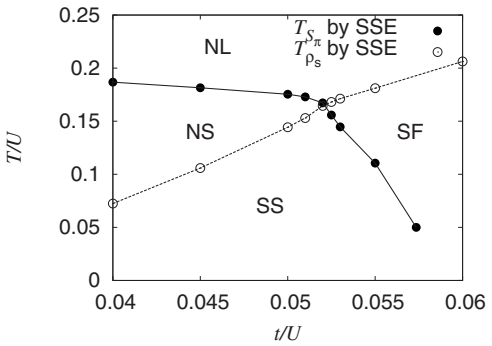

FIG. 6. The t-T phase diagram for $V/U=1/z$ and $\mu/U=0.7$ obtained by SSE. The transition temperatures of the solid state T_{S_π} are plotted by solid circles and those of the superfluid state T_{ρ_s} are plotted by open circles. The lines connect the data points for the guide to the eyes.

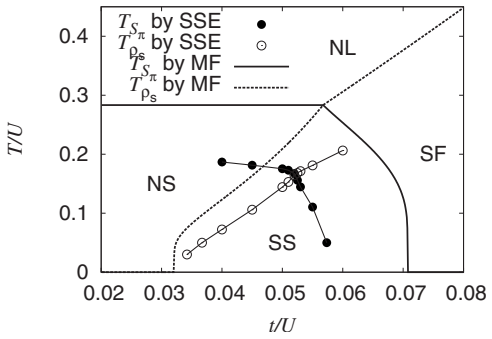

FIG. 8. The t-T phase diagram for $V/U=1/z$ and $\mu/U=0.7$ obtained by MF. The transition temperature of the solid state T_{S_π} is denoted by the thick solid line and that of the superfluid state T_{ρ_s} is denoted by the thick dashed line. We also depict the phase diagram (solid and open circles) obtained by SSE (Fig. 6) for comparison.

successive transitions of superfluid and solid for $(t/U=0.045, \mu/U=0.7)$. As was seen in the SSE simulation, here we find again the suppression of the solid order by the superfluid fraction. Namely, S_π has a cusp at the superfluid transition point. We also depict the phase diagram and compare that to that of SSE (Fig. 8). They show a qualitatively good agreement, e.g., there is the tetracritical point (t_c, T_c) and the critical temperatures T_{S_π} and T_{ρ_s} are suppressed by appearance of the other order as mentioned before.

Let us study the competition between the solid and superfluid orders by analyzing the Ginzburg Landau (GL) free energy. Since the order parameters m and ϕ take small value in the vicinity of the tetracritical point, the GL free energy is expressed as

$$F = am^2 + bm^4 + c\phi^2 + d\phi^4 + hm^2\phi^2. \tag{13}$$

When a becomes zero at $T_{S_\pi}[a \simeq a_0(T-T_{S_\pi})]$ with a positive b, the second-order transition between the normal solid and normal liquid phases takes place, and similarly when c becomes zero at $T_{\rho_s}[c \simeq c_0(T-T_{\rho_s})]$ with a positive d, the second-order transition between the superfluid and normal liquid phases takes place. The fifth term represents the competition between the solid and the superfluid order. If h equals zero, the transition of the solid phase and that of superfluid take place independently at T_{S_π} and T_{ρ_s}, respectively.

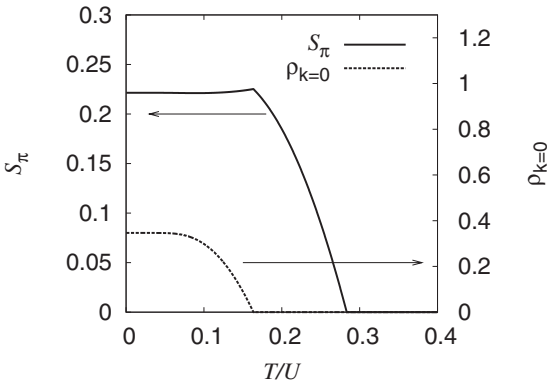

FIG. 7. Temperature dependence of order parameters for $V/U=1/z$, $t/U=0.045$, and $\mu/U=0.7$ obtained by MF. Solid line denotes the solid order parameter and the dashed line denotes the superfluid order parameter.

If h is positive, the presence of the superfluid order lowers the transition temperature of solid. Below the t_c, the solid order emerges first as temperature decreases. Then, the superfluid order appears at the modified transition temperature T'_{ρ_s} which is smaller than the original one

$$T'_{\rho_s} < T_{\rho_s} - \frac{a_0 h/2bc_0}{1 - a_0 h/2bc_0}(T_{S_\pi} - T_{\rho_s}) < T_{\rho_s}. \tag{14}$$

In the same way, the solid order lowers the transition temperature of superfluid. The decrease of the transition temperatures becomes large when h becomes large and this means the shrinkage of the supersolid region. Thus, h represents the competition between the solid and the superfluid orders.

As a final part of this section, we discuss the effect of on-site repulsion on the coexistence of solid and superfluid orders. As has been mentioned, the SS phase does not exist in the ground-state μ-t phase diagram for the hardcore case which corresponds to the limiting case of infinite U. Therefore we expect that the supersolidity is suppressed when the on site repulsion U becomes large. We depict the t-T phase diagram for various values of U in Fig. 9 obtained by MF. Here, we use zV as the unit of energy instead of U because now we want to study the effect of U. In Fig. 9, we find that the SS region becomes narrower as U increases. Finally, the supersolid region disappears completely in the hardcore limit $U \to \infty$, where a first-order transition between solid and superfluid phases takes place. Thus, we conclude that U, i.e., the hardness of the particle, suppresses the coexistence of the two orders.

VI. DISCUSSION AND SUMMARY

We studied properties of supersolid state in three-dimensional extended Bose-Hubbard model by using SSE simulation and MF analysis. First we studied the ground-state phase diagram. There we found the existence of supersolid phase in the region of $\rho < 1/2$. We confirmed that this

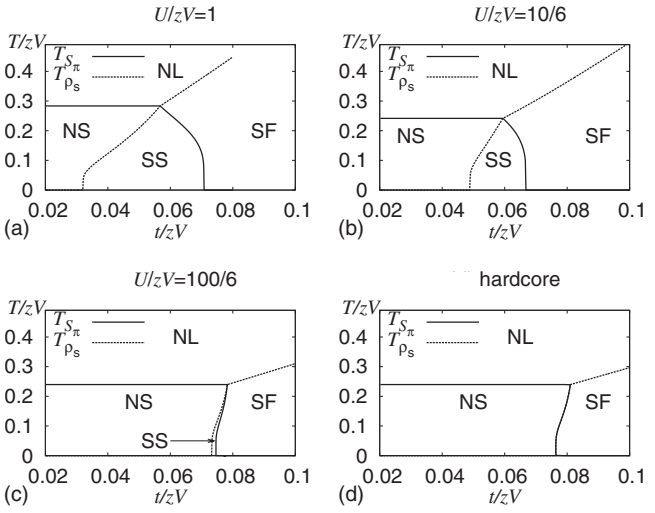

FIG. 9. The dependence of finite temperature phase diagrams on U obtained by MF for a fixed value of $\mu/zV=0.7$. (a) $U/zV=1$, (b) $U/zV=10/6$, (c) $U/zV=100/6$, and (d) hardcore ($U/zV=\infty$).

phase exists in three-dimensional systems in contrast to the cases of one- and two-dimensional cases. Next we studied the properties at finite temperatures. When the system has the supersolid phase in the ground state, the superfluid and solid orders appear successively when the temperature decreases. The strong hopping term (large t) favors the superfluid and the superfluid phase appears at higher temperature in the large t region. On the other hand, in the small t region, the normal solid phase appears first. In both cases we find that the orders of superfluid and solid appear at different temperatures, i.e., successive phase transitions. We find a phase diagram with a tetracritical point and studied the competition between the solid and superfluid orders. By analyzing the dependence of the phase diagram on the on-site repulsion U in particular near the tetracritical point, we find that larger U enhances the competition between two orders and causes the shrinkage of the supersolid region. It would help us to understand how the softness of particles contributes to the realization of the supersolid.

Possibility of realization of the supersolid state on the optical lattice has been discussed recently. The realization of the Bose-Hubbard model in the optical lattice has been discussed.[28] For realization of the supersolid state, the nearest-neighbor repulsive interaction V plays an important role. Mazzarella *et al.*[29] discussed how to introduce the nearest-neighbor interaction. We expect that the parameters of the system can be widely controlled in the optical lattice and there the properties of the phase diagram obtained in this paper will be observed.

ACKNOWLEDGMENTS

The authors would like to thank Hiroshi Fukuyama for his valuable discussions. We also acknowledge useful discussions with Keigo Hijii. The numerical simulations were performed using ALPS applications and libraries (Refs. 18 and 19). This work was partially supported by a Grant-in-Aid for Scientific Research on Priority Areas "Physics of new quantum phases in superclean materials" (Grant No. 17071011) and also by the Next Generation Super Computer Project, Nanoscience Program of MEXT. Numerical calculations were done on the supercomputer of ISSP.

[1] O. Penrose and L. Onsager, Phys. Rev. **104**, 576 (1956).
[2] A. J. Leggett, Phys. Rev. Lett. **25**, 1543 (1970).
[3] E. Kim and M. H. W. Chan, Science **305**, 1941 (2004).
[4] S. Sasaki, R. Ishiguro, F. Caupin, H. J. Maris, and S. Balibar, Science **313**, 1098 (2006).
[5] A. F. Andreev and I. M. Lifshitz, Sov. Phys. JETP **29**, 1107 (1969).
[6] H. Matsuda and T. Tsuneto, Suppl. Prog. Theor. Phys. **46**, 411 (1970).
[7] M. Boninsegni, J. Low Temp. Phys. **132**, 39 (2003).
[8] S. Wessel and M. Troyer, Phys. Rev. Lett. **95**, 127205 (2005).
[9] D. Heidarian and K. Damle, Phys. Rev. Lett. **95**, 127206 (2005).
[10] R. G. Melko, A. Paramekanti, A. A. Burkov, A. Vishwanath, D. N. Sheng, and L. Balents, Phys. Rev. Lett. **95**, 127207 (2005).
[11] M. Boninsegni and N. Prokof'ev, Phys. Rev. Lett. **95**, 237204 (2005).
[12] G. G. Batrouni and R. T. Scalettar, Phys. Rev. Lett. **84**, 1599 (2000).
[13] T. Suzuki and N. Kawashima, Phys. Rev. B **75**, 180502(R) (2007).
[14] P. Sengupta, L. P. Pryadko, F. Alet, M. Troyer, and G. Schmid, Phys. Rev. Lett. **94**, 207202 (2005).
[15] A. W. Sandvik and J. Kurkijärvi, Phys. Rev. B **43**, 5950 (1991).
[16] A. W. Sandvik, Phys. Rev. B **59**, R14157 (1999).
[17] F. Alet, S. Wessel, and M. Troyer, Phys. Rev. E **71**, 036706 (2005).
[18] http://alps.comp-phys.org/
[19] A. F. Albuquerque, F. Alet, P. Corboz, P. Dayal, A. Feiguin, S. Fuchs, L. Gamper, E. Gull, S. Gürtler, A. Honecker *et al.*, J. Magn. Magn. Mater. **310**, 1187 (2007).
[20] E. L. Pollock and D. M. Ceperley, Phys. Rev. B **36**, 8343 (1987).
[21] N. V. Prokof'ev and B. V. Svistunov, Phys. Rev. B **61**, 11282 (2000).
[22] X. Lu and Y. Yu, Phys. Rev. A **74**, 063615 (2006).
[23] A. van Otterlo, K. H. Wagenblast, R. Baltin, C. Bruder, R. Fazio, and G. Schön, Phys. Rev. B **52**, 16176 (1995).
[24] K. Yamamoto and S. Miyashita (unpublished).
[25] V. W. Scarola, E. Demler, and S. Das Sarma, Phys. Rev. A **73**, 051601(R) (2006).
[26] G. G. Batrouni, F. Hebert, and R. T. Scalettar, Phys. Rev. Lett. **97**, 087209 (2006).
[27] K. Binder, Phys. Rev. Lett. **47**, 693 (1981).
[28] D. Jaksch, C. Bruder, J. I. Cirac, C. W. Gardiner, and P. Zoller, Phys. Rev. Lett. **81**, 3108 (1998).
[29] G. Mazzarella, S. M. Giampaolo, and F. Illuminati, Phys. Rev. A **73**, 013625 (2006).